van der Waals interactions between sharp probes and flat sample surfaces

U. Hartmann
Institute for Thin Film and Ion Technology, Forschungszentrum Jülich G.m.b.H., D-5170 Jülich, Federal Republic of Germany
(Received 23 April 1990)

Based on rigorously macroscopic arguments, a theory of van der Waals interactions between probes of various geometries and a flat sample surface is derived. While the spatial resolution of force sensing is shown to depend solely on probe geometry and probe-sample spacing, the magnitude of the force is additionally determined by the dielectric permittivities of probe, sample, and surrounding mediums. Polar immersion liquids considerably reduce van der Waals forces and may cause a transition from attractive to repulsive interactions. Apart from emphasizing some fundamental aspects, the derived results are of certain relevance to long-range scanning force microscopy.

Atomic force microscopy (AFM) has opened the possibility of sensitively mapping forces near sample surfaces.[1] AFM can be used to investigate surfaces of both electrically conducting and nonconducting samples, thus overcoming a major limitation of scanning tunneling microscopy (STM).[2] Depending on the mode of operation many types of forces can be probed, including repulsive contact,[3] frictional,[4] surface tension,[5] electrostatic,[6] magnetostatic,[7] and van der Waals forces.[8–10] In the noncontacting operation mode of scanning force microscopy, van der Waals forces are the sole sources of interaction between clean, electrically neutral, and nonmagnetic probe and sample. The long-range forces can be detected for probe-sample distances of more than 10 nm and may thus be of importance to nondestructive surface profiling applications.[8]

van der Waals (vdW) forces arise from instantaneous moments of otherwise nonpolar atoms or molecules. The quantum fluctuations involved are mostly in the uv range and play an important role in optical dispersion. Calculations of dispersion forces relevant to scanning force microscopy have been based so far on a microscopic approach assuming simple additivity of the atomic contributions.[11] The resulting macroscopic force obtained by straightforward integration over probe and sample atoms can then be separated into a solely geometrical- and a purely material-dependent part. However, since the early work of Lifshitz[12] it is known that this simple microscopic approach does not rigorously characterize the collective nature of macroscopic dispersion interactions.

In the present contribution we derive a theory describing vdW interactions between a sharp probe and a flat sample surface based on macroscopic dielectric properties. The approach accounts for retardation effects as well as for the influence of any dielectric immersion medium surrounding probe and sample. It is shown that a variety of phenomena results from the convolution of geometrical and dielectric properties ignored in previous microscopic theories.

The basic ansatz consists in integrating the extended Lifshitz formula[12,13] for a microscopic probe of rotational symmetry,

$$F(d)=\int_d^\infty \frac{\partial f}{\partial z} G(z-d)dz \ , \tag{1}$$

where F is the dispersion force depending on the distance d between probe and sample. G is the cross-sectional area of the probe depending on the vertical coordinate z. The sample is simply considered as a half-space. The force gradient per unit area of the probe, $\partial f/\partial z$, is then determined by the Lifshitz equation giving the force between individual half-space elements separated by a distance z,

$$f(z)=\frac{\hbar}{4\pi^2 c^3}\int_0^\infty\int_1^\infty p^2\xi^3\epsilon_3^{3/2}\left[\frac{1}{\alpha\exp(x)-1}+\frac{1}{\beta\exp(x)-1}\right]\times dp\,d\xi \ , \tag{2a}$$

using the abbreviations

$$\alpha(p,\xi)=[(\gamma_1+p)(\gamma_2+p)]/[(\gamma_1-p)(\gamma_2-p)] \ , \tag{2b}$$

$$\beta(p,\xi)=\{[\gamma_1+(\epsilon_1/\epsilon_3)p][\gamma_2+(\epsilon_2/\epsilon_3)p]\}\times\{[\gamma_1-(\epsilon_1/\epsilon_3)p][\gamma_2-(\epsilon_2/\epsilon_3)p]\}^{-1} \ , \tag{2c}$$

$$\gamma_j(p,\xi)=[(\epsilon_j/\epsilon_3)-1+p^2]^{1/2} \ , \tag{2d}$$

$$x(p,\xi)=(2\epsilon_3^{1/2}z/c)p\xi \ . \tag{2e}$$

According to Eqs. (1) and (2) the vdW force is determined, apart from the given probe geometry, by the dielectric permittivities ϵ_1,ϵ_2 of the probe and sample as well as ϵ_3 of the surrounding medium.

The apparent obstacle to a straightforward computation of the above formulas is our limited knowledge of the dielectric permittivities involved. The latter provide complete information on the strengths and locations of

the energy-absorption spectra for frequencies from zero to the x-ray range. Fortunately, partial data combined with general constraints sharply restrict ambiguity in using ϵ to calculate dispersion forces: ϵ has to be determined only on the imaginary frequency axis, $\omega=i\xi$, where $\epsilon(i\xi)$ is real and monotonic decreasing from the static value $\epsilon(\xi=0)$ to $\epsilon(\xi\rightarrow\infty)=1$. Split into successive frequency regimes, $\epsilon(i\xi)$ is then given by simple relations only envolving some spectral parameters,

$$\epsilon(i\xi)=1+\sum_m \frac{c_m}{1+\xi/\omega_m}+\sum_n \frac{c_n}{1+(\xi/\omega_n)^2} , \tag{3a}$$

where the first term describes the Debye rotational relaxation and the second the Lorentz harmonic oscillation. $\omega_{m,n}$ are characteristic resonance frequencies and $c_{m,n}$ are the corresponding absorption constants given for almost all materials of interest from tables of dielectric data. Equation (3a) provides some description of $\epsilon(i\xi)$ for dielectric materials through the visible to the near-uv range.

In dielectric crystals only the band transitions and the electronic plasma oscillations in the valence band significantly contribute to the dispersion forces,[14]

$$\epsilon(i\xi)=1+\sum_n \omega_{pn}^2/(\omega_n^2-\xi^2) , \tag{3b}$$

where ω_{pn} is the plasma frequency of the respective absorption center of type n. However, in the far-uv and soft-x-ray region, $\epsilon(i\xi)$ always has the limiting form

$$\epsilon(i\xi)=1+\omega_p^2/\xi^2 , \tag{3c}$$

where ω_p is the free-electron plasma frequency.[15] A suitable interpolation scheme for the intermediate range between Eqs. (3b) and (3c) has been suggested by Ninham and Parsegian.[16] For metals one simply obtains

$$\epsilon(i\xi)=\omega_p^2/\xi^2 , \tag{3d}$$

for the relevant IR regime, whereas for smaller frequencies $\epsilon(i\xi)$ is directly related to the electrical conductivity σ,

$$\epsilon(i\xi)=\sigma/(\epsilon_0\xi) . \tag{3e}$$

Equations (1)–(3) now permit the calculation of vdW forces between probe and sample for any dielectric materials involved. However, the complex convolution of geometrical and dielectric contributions can only be evaluated by computer-intensive numerical methods. To investigate the effect of probe geometry in more detail, we choose a probe-sample system of two identical metals in vacuum, i.e., $\epsilon_1=\epsilon_2$, given according to Eqs. (3d) and (3e), and $\epsilon_3=1$. The probe is approximated by a cylinder, a paraboloid, and a cone, respectively. The resulting vdW forces depending on the probe-sample separation are shown in Fig. 1. For small separations the interaction is completely nonretarded. Analytical expansion of the formulas shows that forces are simply given by

$$F_n(d)=g_n H_n/d^n , \tag{4a}$$

where g_n is a constant solely depending on the actual probe geometry.[17] H_n is the nonretarded Hamaker constant depending on the dielectric permittivities $\epsilon_j(i\xi)$ of all media involved,

$$H_n=\frac{3\hbar}{4\pi}\sum_{n=1}^{\infty}\frac{1}{n^3}\int_0^{\infty}d\xi\left[\frac{\epsilon_1-\epsilon_3}{\epsilon_1+\epsilon_3}\right]^n\left[\frac{\epsilon_2-\epsilon_3}{\epsilon_2+\epsilon_3}\right]^n . \tag{4b}$$

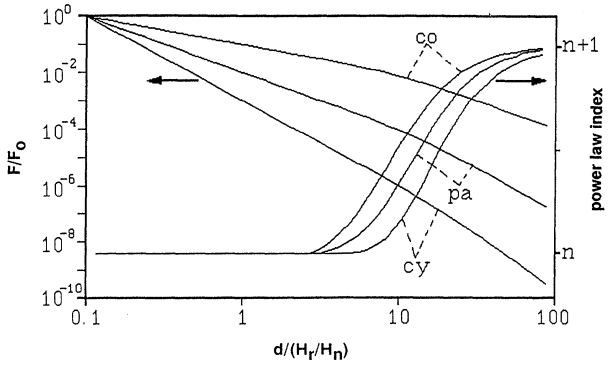

FIG. 1. van der Waals forces as a function of the probe-to-sample distance. H_n and H_r denote the nonretarded and retarded Hamaker constants, respectively. Probe and sample consist of typical metals and are surrounded by vacuum. The curves correspond to a cylindrical (cy), a paraboloidal (pa), and a conical (co) probe model, respectively. During transition from the nonretarded to the retarded limit the power-law indices exhibit a continuous increase from n to $n+1$, with $n=3$ (cy), $n=2$ (pa), and $n=1$ (co).

For increasing probe-sample separation, interactions are affected by retardation of the radiation field[12] leading to a monotonic increase of the power-law index n in Eq. (4a), see Fig. 1. In the completely retarded limit, the force is given by

$$F_r(d)=g_r H_r/d^{n+1} , \tag{5a}$$

with a geometrical constant g_r (Ref. 17) and the retarded Hamaker constant

$$H_r=\frac{3\hbar c}{16\pi^2}\frac{1}{\epsilon_{30}^{1/2}}\sum_{n=1}^{\infty}\frac{1}{n^4}\int_1^{\infty}\frac{dp}{p^2}\left[\frac{1}{\alpha_0^n}+\frac{1}{\beta_0^n}\right] , \tag{5b}$$

where $\alpha_0(\epsilon_{j0},p)$ and $\beta_0(\epsilon_{j0},p)$ are given by Eqs. (2b) and (2c) using the static dielectric constants ϵ_{j0}. For the probe geometries considered in Fig. 1, the power-law indices are given by $n=3$ for the cylinder, $n=2$ for the paraboloid, and $n=1$ for the cone, respectively. The limiting formulas (4a) and (5a) are consistent with the microscopic theory.[11] However, the Hamaker constants H_n and H_r as well as the geometry- and material-dependent transition to the retarded regime can only be evaluated by the rigorously macroscopic procedure.

Due to the long-range manifestation of the forces, directly reflected by Eqs. (4a) and (5a), the "effective detector volume" of the probe is determined by the mesoscopic geometry near the probe apex. To estimate the actual lateral resolution obtained upon laterally scanning the sample surface, the variation of the force gra-

dient $\partial F/\partial z$ along the probe axis is relevant. This variation is shown in Fig. 2 for different geometries in the nonretarded and retarded limits. While the cylinder exhibits a monotonic decrease of $\partial F/\partial z$ along its axis, the paraboloid and cone show a shift of $(\partial F/\partial z)_{\max}$ along their axes. The lateral resolution R of the probe is then characterized by its diameter in the effective center of interaction which is determined by the location of $(\partial F/\partial z)_{\max}$. In this way we obtain for the nonretarded limit[18]

$$R_{\rm pa}=[2l_{xy}/(3l_z)^{1/2}]d^{1/2}\ , \tag{6a}$$

$$R_{\rm co}=2\tan\varphi d\ , \tag{6b}$$

for a paraboloid with semiaxes l_{xy} and l_z, and for a cone with half-angle of aperture φ, respectively. The above results show that the loss in spatial resolution with increasing working distance is smaller for a paraboloidal probe than for a conical one. For the cylindrical probe R is constant and given by the probe diameter. It should be emphasized that lateral resolution does not depend on any material parameter, but is determined by the probe geometry and working distance. Employing probe dimensions typical for AFM tips, Eqs. (6) clearly confirm experimental results according to which the achieved lateral resolution is approximately equal to the probe-sample distance if the latter is in the nm range.

According to Eqs. (2), any immersion medium should have a distinct effect on the dispersion force between probe and sample in terms of a dielectric contribution $\epsilon_3(i\xi)$. In particular, highly polar H-bonding liquids are known to considerably modify vdW forces.[10,11] Apart from a dispersion contribution such liquids exhibit a solely entropic zero-frequency contribution to the vdW interaction which includes Debye and Keesom relaxation of the polar molecules. This latter contribution acts like an additive term of $H_e/(6\pi z^3)$ to $f(z)$ in Eq. (2a). The entropic Hamaker constant is given by

$$H_e=\tfrac{3}{4}kT[(\epsilon_{10}-\epsilon_{30})/(\epsilon_{10}+\epsilon_{30})] \times[(\epsilon_{20}-\epsilon_{30})/(\epsilon_{20}+\epsilon_{30})]\ , \tag{7}$$

where kT denotes the thermal energy and ϵ_{j0} the static dielectric constants of all media involved. To systematically check the effect of immersion in polar liquids, vdW forces have been calculated for a SiO_2-metal combination of probe and sample. However, all solutions of the theory are invariant to an exchange of probe and sample material. Some characteristic results are summarized in Fig. 3. Polar liquids considerably reduce the magnitude of the vdW force with respect to the vacuum level. For H_2O, H_2O_2, and glycol, a transition from attractive to repulsive interactions is expected at large probe-sample separations. This is due to a negative entropic contribution which does not suffer retardation and thus exceeds the dispersion contribution at distances in the 100-nm range. For glycerol and formamide the entropic contribution is dominant at any probe-sample separation resulting in a solely repulsive interaction.

An important limitation of scanning force microscopy for being a nondestructive tool is the magnitude of the force applied by the probe on the surface to be imaged.[19] Recent calculations suggest that loading forces should not exceed 10^{-11} N for organic samples[20] and 10^{-9} N for crystalline surfaces.[21] In conclusion, the present calculations confirm that, apart from suppressing parasitic surface tension forces,[10] immersion of the probe-sample system in highly polar liquids can reduce vdW forces up to more than two orders of magnitude at small probe-sample distance. Additionally, by an appropriate choice of the immersion medium, forces can be externally determined to be either attractive or repulsive. Zero-force points obtained for some immersion media may be of importance to long-range operation modes like Coulomb charge[6] or magnetic force[7] microscopy.

Finally, it is emphasized that the derived theory is predominantly focused on an analysis of the basic fundamentals of vdW interaction in a particular system, rather than on a rigorously realistic characterization of the ex-

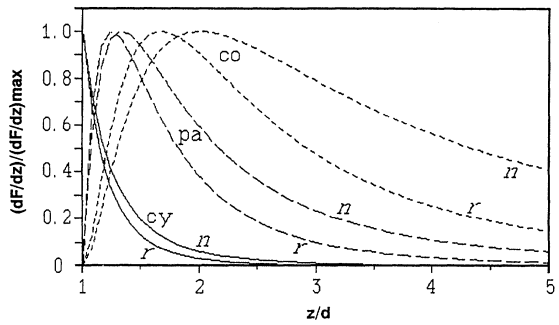

FIG. 2. Variation of the force gradient within various probes along their symmetry axes. $z/d=1$ defines the probe apex separated by a distance d from the sample surface. The curves correspond to a cylinder (cy), a paraboloid (pa), and a cone (co) in the nonretarded (n) and retarded (r) limits of interaction, respectively.

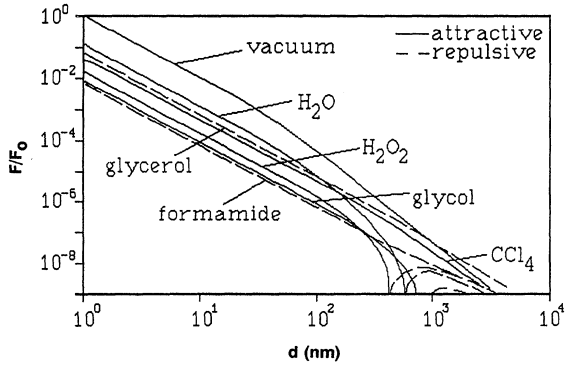

FIG. 3. Variation of van der Waals forces with increasing probe-sample separation for a SiO_2-metal combination of probe and sample in various polar immersion media. The AFM probe is assumed as a paraboloidal tip. Forces are normalized with respect to the vacuum level at a probe-sample distance of 1 nm.

perimental situation in scanning force microscopy. In particular, the presently detectable force range clearly restricts an experimental verification of those phenomena related to retardation effects of the radiation field between probe and sample for separations in the 100-nm range. On the other hand, for working distances in the nm range, vdW forces are clearly detectable by experiment. However, for this case the relevant interactions are generally masked by other types of probe-surface interactions, by the surface topology, by surface contaminations, and by an inhomogeneous near-surface dielectric behavior of the involved media. Thus, the present theory should clearly be considered as a somewhat idealized characterization of the basic geometry and material dependence of vdW interactions in a particular probe-sample system.

Valuable discussions with C. Heiden are gratefully acknowledged.

[1]G. Binnig, Ch. Gerber, and C. F. Quate, Phys. Rev. Lett. **56**, 930 (1986).

[2]G. Binnig, H. Rohrer, Ch. Gerber, and E. Weibel, Phys. Rev. Lett. **50**, 120 (1983).

[3]O. Mati, H. O. Ribi, B. Drake, T. R. Albrecht, C. F. Quate, and P. K. Hansma, Science **239**, 50 (1988).

[4]C. M. Mate, G. M. McClelland, R. Erlandsson, and S. Chiang, Phys. Rev. Lett. **59**, 1942 (1987).

[5]R. Erlandsson, G. M. McClelland, C. M. Mate, and S. Chiang, J. Vac. Sci. Technol. A **6**, 266 (1988).

[6]J. E. Stern, B. D. Terris, H. J. Mamin, and D. Rugar, Appl. Phys. Lett. **53**, 2717 (1988).

[7]Y. Martin and H. K. Wickramasinghe, Appl. Phys. Lett. **50**, 1455 (1987).

[8]Y. Martin, C. C. Williams, and H. K. Wickramasinghe, J. Appl. Phys. **61**, 4723 (1987).

[9]G. M. McClelland, R. Erlandsson, and S. Chiang, Rev. Prog. Quantum Nondestruc. Eval. **6**, 1307 (1987).

[10]A. L. Weisenhorn, P. K. Hansma, T. R. Albrecht, and C. F. Quate, Appl. Phys. Lett. **54**, 2651 (1989).

[11]J. N. Israelachvili, *Intermolecular and Surface Forces* (Academic, London, 1985).

[12]E. M. Lifshitz, Zh. Eksp. Teor. Fiz. **29**, 94 (1955) [Sov. Phys.—JETP **2**, 73 (1956)].

[13]I. E. Dzyaloshinskii, E. M. Lifshitz, and L. P. Pitaevskii, Zh. Eksp. Teor. Fiz. **37**, 229 (1959) [Sov. Phys.—JETP **37**, 161 (1960)].

[14]J. Visser, in *Surface and Colloid Science,* edited by E. Matijevic (Wiley, New York, 1976).

[15]L. D. Landau and E. M. Lifshitz, *Electrodynamics of Continuous Media* (Addison-Wesley, Reading, MA, 1960).

[16]B. W. Ninham and V. A. Parsegian, J. Chem. Phys. **52**, 4578 (1970).

[17]$g_n = 1_{xy}^2/6$ and $g_r = \pi l_{xy}^2$ for a cylinder of radius l_{xy}. $g_n = 1_{xy}^2/(12 l_z)$ and $g_r = \pi l_{xy}^2/(3 l_z)$ for a paraboloid with semiaxes l_{xy} and l_z. $g_n = (\tan^2\varphi)/6$ and $g_r = (\pi/3)\tan^2\varphi$ for a cone with half-angle of aperture φ.

[18]In the retarded limit R_{pa} is reduced by a factor of $\sqrt{3}/2$ and R_{co} by a factor of $\frac{2}{3}$. However, these corrections are without experimental relevance since the retarded low-force regime is inaccessible to vdW microscopy.

[19]J. B. Pethica and W. C. Oliver, Phys. Scr. **T19**, 61 (1987).

[20]B. N. J. Persson, Chem. Phys. Lett. **141**, 366 (1987).

[21]F. F. Abraham, I.P. Batra, and S. Ciraci, Phys. Rev. Lett. **60**, 1314 (1988).